Geophysical Research Letters

RESEARCH LETTER
10.1029/2023GL106868

The Effect of Stress on Paleomagnetic Signals: A Micromagnetic Study of Magnetite's Single-Vortex Response

T. L. North[1], A. R. Muxworthy[1,2], W. Williams[3], T. M. Mitchell[2], G. S. Collins[1], and T. M. Davison[1]

[1]Department of Earth Science and Engineering, Imperial College London, London, UK, [2]Department of Earth Sciences, University College London, London, UK, [3]School of GeoSciences, University of Edinburgh, Edinburgh, UK

Key Points:

- Single-vortex particles' net magnetization rotates toward the compression axis when subjected to differential stress
- Single-vortex particles display the opposite response to compressional stress compared to single-domain particles
- Stress fields of only ∼100 MPa are required to alter paleomagnetic signals, lower than previously predicted

Supporting Information:

Supporting Information may be found in the online version of this article.

Correspondence to:

A. R. Muxworthy,
adrian.muxworthy@imperial.ac.uk

Citation:

North, T. L., Muxworthy, A. R., Williams, W., Mitchell, T. M., Collins, G. S., & Davison, T. M. (2024). The effect of stress on paleomagnetic signals: A micromagnetic study of magnetite's single-vortex response. *Geophysical Research Letters*, *51*, e2023GL106868. https://doi.org/10.1029/2023GL106868

Received 23 OCT 2023
Accepted 2 JAN 2024

Abstract In this study we use micromagnetic modeling to show that the magnetizations of magnetically single-vortex particles rotate toward the stress axis on the application of a differential compression stress. This is the exact opposite response to magnetically single-domain particles, which previously provided the theoretical underpinning of the effect of stress on the magnetic signals of rocks. We show that the magnetization directions of single-vortex and equant single-domain particles are altered by much lower stresses than previously predicted, c.f., 100 versus 1,000 MPa; where a change in magnetization is defined as a rotation of >3° after the removal of stress. The magnetization intensity of assemblages also drops by ∼20%–30% on the application and removal of stress of ∼100 MPa. Given that single-vortex particles are now thought to dominate the magnetization of most rocks, future studies should account for paleomagnetic directional uncertainties and potential underestimation of the ancient magnetic field intensity.

Plain Language Summary Magnetic minerals in rocks can record and retain magnetic information for millions of years. This magnetic information helps us to understand processes like plate tectonics and geomagnetic field behavior in the past. When rocks experience compressional forces, these affect the magnetization of the magnetic minerals within them, potentially altering this magnetic information. Previous theoretical studies of the affect of stress on magnetization used analytical theory, and predicted that stresses of >1,000 MPa are required to alter a rock's otherwise stable magnetization. We show that much lower stresses of only ∼100 MPa are required to compromise magnetic recordings in rocks. The reason for this is a change in our understanding of rock magnetic systems. Previous analytical models were for elongated particles <100 nm in size, as these were thought to be the primary carriers of stable magnetization in minerals. We now know that larger particles can retain stable magnetic recordings to high temperatures over geological time. This study shows that the magnetization of these particles are less stable than smaller particles when stresses are applied. This suggests that common geological processes such earthquakes might provide sufficient near-surface stress to remagnetize rocks close to the fault zone, leading to a paleo-stress recording.

1. Introduction

The paleomagnetic field recorded by rocks and meteorites is central to understanding many key events in the history and evolution of Earth and the Solar System, for example, inner core nucleation (e.g., Biggin et al., 2015). Notwithstanding the many great successes, paleomagnetic studies have largely ignored the potential for "low" levels of stress (<1 GPa) to alter paleomagnetic signals, even though there are many examples where such stresses are known to influence the magnetization, for example, seismically active faults (e.g., Elhanati et al., 2020). Why have low stresses been ignored? Since the work of Néel (1949), it has been assumed that on geological timescales the particles carrying the magnetic remanence are magnetically uniform, that is, so-called single domain (SD) particles which are ≲80 nm for magnetite (Muxworthy & Williams, 2006). Larger particles, which contain single vortex (SV) and multi-vortex magnetic domain structures (∼80 to ∼10,000 nm), although ubiquitous in rocks, were thought to be less reliable magnetic recorders over geological timescales and thus paleomagnetically less significant. However, the behavior of these SV particles has, until recently, been hard to quantify due to their highly non-linear behavior, which makes modeling challenging, and their small size, which has made magnetic imaging problematic. Even larger particles (>10 μm), known as multidomain (MD), whose size makes them easier to directly observe, have been demonstrated as paleomagnetically unreliable.

Néel (1949) theory primarily addresses the effect of temperature on magnetic stability of small SD particles on geological timescales. It was thought that SD signals dominated paleomagnetic records, and so subsequent theories that attempted to account for the effect of stress on the magnetization of rocks focused mostly on these types of particles (e.g., Dunlop et al., 1969; Hodych, 1976, 1977). From theoretical calculations for randomly oriented SD particles, it is easy to show that stresses in excess of 1 GPa are needed to demagnetize or re-magnetize stable SD remanences. However, these calculations are not entirely supported by experimental work, most of which was conducted in the 1960–1980s (e.g., Hamano et al., 1989; Kapička, 1992; Nagata, 1971; Schmidbauer & Petersen, 1968) although there are more recent studies (e.g., Volk & Feinberg, 2019; Volk & Gilder, 2016). Nagata's 1960s experiments—succinctly summarized in Nagata (1971)—demonstrated that magnetic remanences of rocks could be irreversibly altered by stresses of just tens of MPa. This disconnect between theory and observation was largely ignored or attributed to paleomagnetically "unstable" larger particles (e.g., Volk & Feinberg, 2019) or lower stability due to the presence of titanium (e.g., Sato et al., 2021).

We now know that the reliance on SD theory in interpreting paleomagnetic signals is wrong. A combination of new nanometric imaging protocols (e.g., Almeida et al., 2016) and new numerical models (Nagy et al., 2017; Ó Conbhuí et al., 2018), has shown that it is actually SV particles that carry the most "stable" magnetic remanences on geological timescales, not SD particles (Nagy et al., 2022). This has led to a step-change in our understanding of magnetic recordings in natural systems.

Given this new understanding of rock magnetic recordings, and the mismatch between the theoretical predictions and observations of the effect of stress on the magnetization of rocks, in this paper, we study the effect of uniaxial compressive stress on the magnetic behavior of SV particles using numerical micromagnetic models. We consider uniaxial differential stresses rather than hydrostatic stresses, as it is differential stresses that are known to cause significant changes to the magnetization; rocks have been shown experimentally to be almost independent of hydrostatic stresses at crustal stresses (Kapička, 1992). We have implemented uniaxial stress into the micromagnetic code MERRILL (Ó Conbhuí et al., 2018), and use this model to understand and quantify how stress will effect magnetic domain structures and remanent magnetizations.

2. Methods

We have modeled the effect of peak compressional stress on the magnetization of truncated-octahedral magnetite particles at room temperature as a function of particle size for the following equivalent-volume spherical diameters (EVSD); 50, 80, 100, 150, and 200 nm), and for three different prolate aspect ratios (ARs): 0%, 50%, and 100% elongation, that is, AR = 1.0, 0.67, and 0.5 respectively, using the micromagnetic software package MERRILL (Ó Conbhuí et al., 2018). MERRILL uses finite element meshes, which were generated using the meshing package Coreform Cubit (Coreform LLC, 2017). In the models, it is desirable to have the maximum mesh size no greater than the material's exchange length, which for magnetite is 9 nm. All our model geometries were meshed at 8 nm.

We essentially considered a dynamical stress where the magnetite particles are not in equilibrium, which this is equivalent to a shock wave passing through a material. This first-order approach allows us to ignore magnetostrictive effects (Fabian & Heider, 1996). We simulate a stress field at a given angle by applying an additional energy term to the anisotropy (E_σ) to MERRILL (Dunlop et al., 1969),

$$E_\sigma = \frac{3}{2}\lambda_s \sigma V \sin^2\theta \tag{1}$$

where λ_s is the isotropic magnetostriction constant, V the volume, and θ is the angle between the magnetization and the direction along which the stress is applied. In addition to the standard room-temperature parameters for magnetite included in Ó Conbhuí et al. (2018), we used a value of $\lambda_s = 4.75 \times 10^{-5}$ (Moskowitz, 1993).

From an initial state, we determine the new magnetization structure under the influence of a compressional stress (the "stressed state"), before removing the stress field and determining the new magnetization structure (the "zero-stress state"). We repeat this for increasing stresses up to 3,000 MPa, using the previous "zero-stress state" as the initial state. At these relatively low stresses, the effect of heating is predicted to be minimal, that is, <10°C (North, Collins, et al., 2023), therefore we do not include temperature variation in our models. To capture the response of a random distribution, we repeated this for 20 orientations over an octant of a sphere

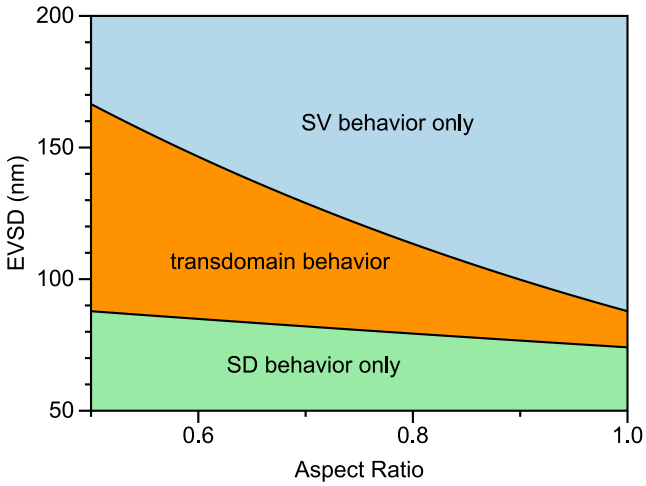

Figure 1. Summary of the model groupings defined by behavior in the zero-stress-state models plotted on a graph of equivalent volume spherical diameter (equivalent-volume spherical diameters [EVSD]) and aspect ratio (AR): single domain behavior only, single vortex behavior only, and transdomain behavior where the effect of stress is to nucleate/denucleate vortex cores. This graph was determined from all the modeled particles, that is, 50 ≤ EVSD ≤ 200 nm, and 0.5 ≤ AR ≤ 1.0.

determined using a Fibonacci distribution as we have done previously (e.g., Nagy et al., 2022).

3. Numerical Results for Individual Particles

Critical to the response of a magnetic structure to the application of stress in the micromagnetic model is the initial magnetization state. Initial SD magnetizations were aligned with either an easy magnetocrystalline axis (<111> for magnetite) or the elongation (long) axis, while the core of the initial SV states were aligned with magnetite's easy <111> or hard <100> axes, the short or long ellipsoid axes, an intermediate direction midway between an easy magnetocrystalline axis and a short ellipsoid axis or curved vortex cores which connect easy-axes crystal faces (see Supporting Information S1 for images of these initial structures). These initial states are all local-energy minima (LEM), though some have higher energies than others, for example, in the equant 80 nm particle we consider both initial SD (higher energy) and SV (lower energy) states aligned along both hard and easy magnetocrystalline anisotropy axes. All these initial states have been previously documented in the literature (e.g., Fabian et al., 1996; Nagy et al., 2019).

The results for individual particles fall into three groups: (a) where the particles are in SD states at all times for the zero-stress-state solutions, (b) SV states at all times for the zero-stress-state solutions, and (c) where some of the particles for a given size and AR change domain state in response to stress by nucleating/de-nucleating vortex cores, that is, transdomain processes (Dunlop et al., 1994); the groupings are summarized in Figure 1 below. We consider the three cases separately.

3.1. Exclusively SD States

All the 50 nm particles (0.5 < AR < 1.0) and the 80 nm model with AR = 0.5, were in the SD state at all times within the stress-cycling models. The effect of stress is to rotate the magnetic moments into the plane of the stress, that is, perpendicular to the compressional stress axis, causing a change in net magnetization away from the stress field into the stress plane. On relaxing the stress, the magnetization rotates toward the closest easy axis (Figure 2). For equant particles this is one of the four easy magnetocrystalline axes, for the elongated particles this is the long axes. Depending on the initial orientation of the magnetization with respect to the stress axis and the size of the applied stress, the initial magnetization state, that is, direction, is usually recovered after removal of the stress field. That is, the response to stress for most SD particles is reversible, with only a few particles displaying irreversible behavior on removal of stress; 4 from 80 models. Such irreversible behavior is seen Figures 2a–2c, for an equant 50 nm EVSD particle where the net magnetization of the particle flips from one easy axis <111> to another on the relaxation of stress. The chance of irreversible behavior increases with higher order anisotropies, that is, equant particles are much more likely to be affected by stress than elongated particles, and random population of equant particles will demagnetize more than a similar population of elongated particles. The response of the SD models for the elongated particles, that is, AR < 1, is very similar to that expected from analytical SD theory (e.g., Hodych, 1976, 1977), with any variations due to configurational anisotropy (Williams et al., 2006) or multi-axial anisotropy not captured by analytical SD theory of uniaxial particles.

3.2. Exclusively SV States

Here we consider particles which remain in an SV state under zero-stress conditions after simulated application of stress. This groups consists of equant particles for the 100–200 nm EVSD models, the 150 and 200 nm models for AR = 0.67 and the 200 nm for AR = 0.5 (Figure 1). In SV systems the net magnetic moment is carried in the core direction (Williams & Dunlop, 1989). On application of a stress field the core rotates into the direction of the stress field (Figures 2g–2i), this is because in SV systems the magnetic moments in the shell of the SV particles rotate to be perpendicular to the stress field (Equation 1). This means that the SV core, which carries the net magnetic moment, rotates into the direction of the stress field. The SV core diameter (as represented by

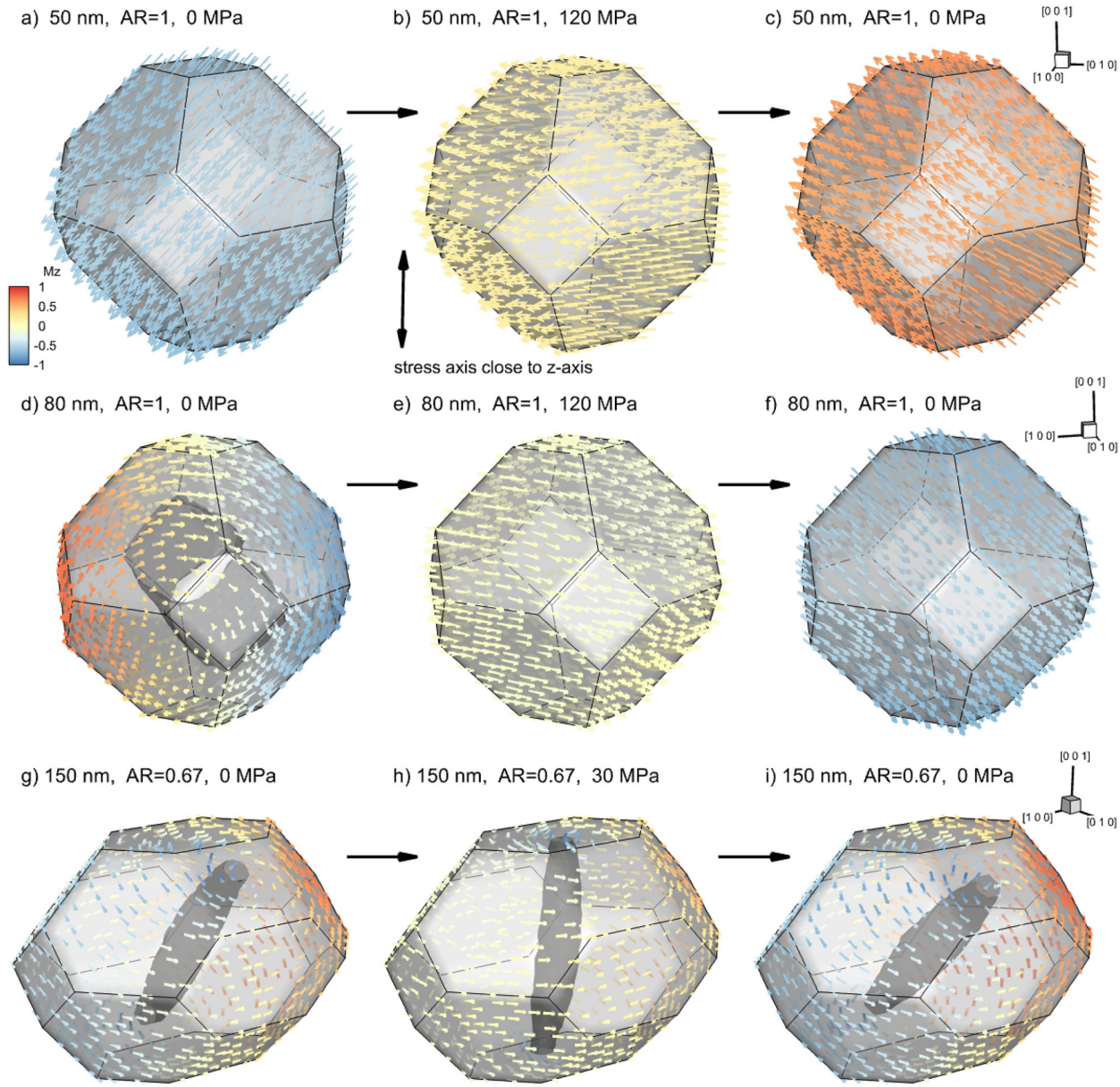

Figure 2. Examples of the effect of stress on micromagnetic structures. In (a–c) a 50 nm equivalent-volume spherical diameters (EVSD) particle with aspect ratio (AR) = 1: (a) for the initial state, (b) under compressional stress of 120 MPa applied close to <001>, that is, ∼10° from the *z*-axis, and (c) in 0 MPa after relaxing the stress applied in panel (b). Figures (d–f) are for a 80 nm EVSD equant (AR = 1) particle under identical conditions to the 50 nm EVSD particle in panels (a–c). In (d) the structure contains a vortex core, which is highlighted by an isosurface at 95% relative helicity. Figures (g–i) are for a 150 nm EVSD particle with AR = 0.67, where (h) is under a compression stress of 30 MPa aligned in the same directions at (b, e), and (i) is the micromagnetic structure after releasing the 30 MPa stress shown in panel (h). Panels (g–i) all have their vortex cores highlighted in an identical manner to panel (d). The arrows in all the figures are colored by their alignment with respect to the *z*-axis. The orientations of each set of models are shown in panels (c, f, and i). Arrow density has been reduced for clarity.

the 95% relative helicity isosurface) narrows on the application of stress, before broadening after the removal of the stress (Figures 2h and 2i). For high stresses, the particles become SD under stress. Similar behavior was found for both the equant and elongated particles. To quantify the effect of stress we define a critical stress value σ_c as the stress required to rotate the magnetization of the post-stress, zero-stress-state solution ≥3°. σ_c depends strongly on the applied stress angle with respect to the crystallographic axes, giving rise to a distribution of σ_c for an initial magnetization state (Figure 3). σ_c also depends strongly on the initial magnetization domain state orientation, for example, for the 200 nm EVSD AR = 0.67 models if the vortex core is initially aligned along the short axis, $\sigma_c \sim$ 10–20 MPa, but if the core is aligned with the long axis, $\sigma_c \sim$ 100–200 MPa.

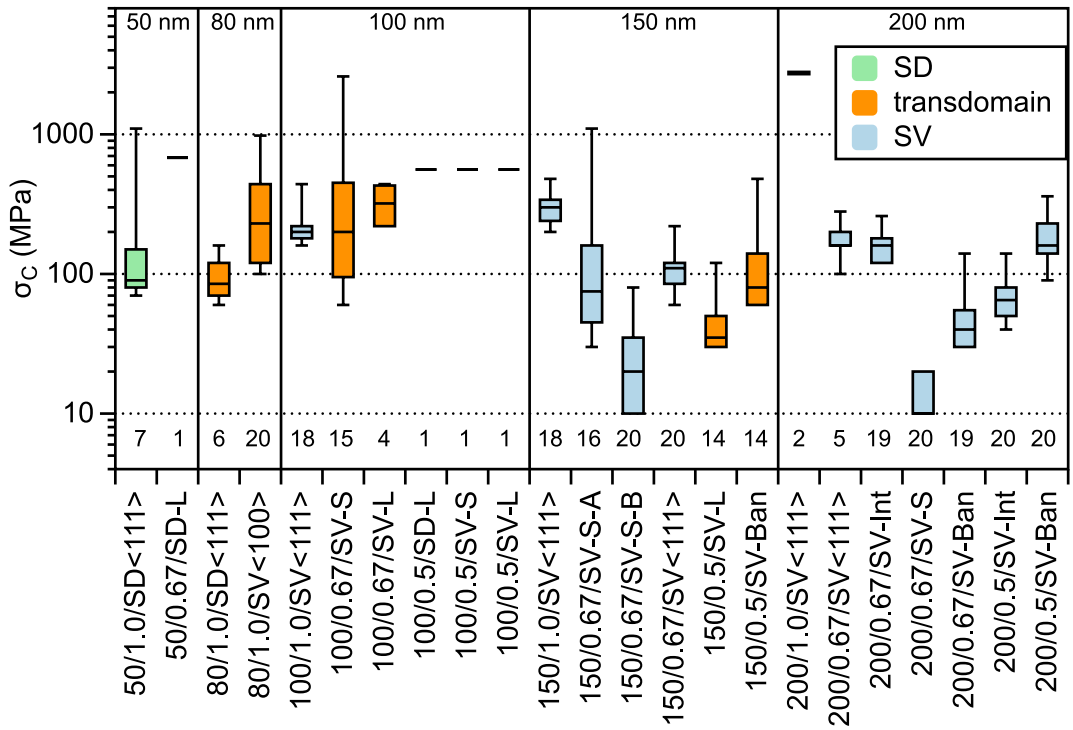

Figure 3. A whisker plot (first and third quartile, plus range and median) of the critical stress σ_c required to rotate the net remanent magnetization vector of a particle >3° from the original magnetization for each initial magnetization state. Each initial state was subjected to stresses oriented over 20 direction directions over an octant chosen using a Fibonacci distribution. Of these 20 models a number (shown immediately above the *x*-axis) yielded σ_c values, which were used to determine the distribution. The initial starting states are shown below the *x*-axis, and are described by equivalent-volume spherical diameters size in nm, followed by the aspect ratio, that is, 1.0, 0.67 or 0.5, and finally a summary of the initial state, that is, either SD or SV for single domain or single vortex, followed by the SD or SV-core orientation, described by one of the four variations: (1) the magnetocrystalline easy "<111>" or hard "<100>" axes, (2) for prolate particles the short "S" or long "L" axes, (3) intermediate "Int" where the SV core is between the short or long axes, and (4) banana "Ban" where the SV core is curved. The whisker plots have been colored by whether the behavior in the remanence state is exclusively SD or SV, or transdomain behavior is observed as stress is applied and released. Not all the initial states yielded a σ_c value and are not depicted, that is, 50/0.5/SD-L, 80/0.67/SV-L, and 80/0.5/SD-L. In the three groupings, for the SD group, nine models from 80 yielded a σ_c value, with 76/200 for the transdomain models and 179/240 for the SV models.

The effect of stress on SV particles is the opposite to that predicted in SD particles, that is the net magnetization of a particle rotates toward the stress direction, whilst SD particles point away (c.f., Figures 2b and 2h). However, similar to the SD particle behavior, SV particles display various degrees of irreversible behavior depending on the controlling anisotropy, that is, magnetocrystalline anisotropy in the case of equant particles or shape anisotropy for the elongated particles. The equant particles, with eight easy directions, display more irreversible behavior than the elongated particles with uniaxial behavior.

3.3. Transdomain Particles

Depending on both particle size and AR, there are particles for which both SD and SV states are energetically possible in the absence of stress, that is, these particles can occupy either SD or SV remanence states depending on their history (Enkin & Williams, 1994; Muxworthy & Williams, 2006). In the particle size range modeled in this study, this phenomena was observed from the 80 nm equant models to the 150 nm elongated particles (AR = 1, Figure 1). The application of stress fields to such particles is sufficient for particles to nucleate vortex cores (SD → SV) or denucleate vortex cores (SV → SD), depending on stress magnitude and axis orientation. We term this "transdomain" behavior, as it is similar to the transdomain behavior reported in thermal micromagnetic models (Dunlop et al., 1994).

The effect of applied uniaxial compressive stress is to align the magnetic moments into the plane of the stress axis (Figures 2d–2f). This can be stable for both SD and SV states depending on the relative orientation of the

stress axis and the particle elongation axis, that is, compressive stress does not automatically form a SD state. In our models there was a preference for denucleation over nucleation of vortex cores (Figures 2 and 3); however, our initial magnetization states were heavily biased toward SV structures as this was our main interest. The stress fields required to cause transdomain processes as indicated by σ_c where generally >100 MPa, and on average higher than that observed for pure SV rotations (Figure 3).

4. Discussion

The response of the particles we have modeled fall into essentially two behaviors; rotation of an SD moment away from the stress axis, or the rotation of the net SV magnetization toward the stress axis (Figure 2). These responses are due to the majority of the magnetic moments in each domain state rotating into the plane of the compressional uniaxial stress governed by Equation 1. There are also transdomain effects, which complicate the behavior, as the net response to compressional stresses are to rotate the magnetization toward or away from the stress axis depending the initial domain state. The transdomain processes only occur in a narrow range of models (Figure 1) close to the AR-dependent SD to SV transition size (Muxworthy & Williams, 2006). However, these processes are also likely to occur in much larger multidomain particles, that is, >1 μm not considered in this study.

The critical stress σ_c is used to identify a change in the zero-stress magnetization state after the stress is released (Figure 3), and is defined by a >3° change in the net magnetic moment direction from the initial magnetization state direction. σ_c depends on particle size, AR and, importantly, the stability of the initial state. For example, for the 150-nm models with AR = 0.67, the SV "B" state aligned on the short axis has a lower σ_c value than an SV state aligned with the <111> direction (Figure 3). This is expected, as although the short-axis SV "B" state is an LEM state, it has a lower stability compared to the long-axis SV "A" state (Nagy et al., 2019). Generally, the SD and transdomain states had both higher σ_c values than the SV states, and a greater number of angles that yielded σ_c values (Figure 3), suggesting SV structures are more likely to be affected by low levels of differential compressional stress, that is, ≤100 MPa compared to SD states.

4.1. Assemblages of Samples

To the Earth Scientist attempting to retrieve ancient recordings that evidence past geological events, there are essentially two key areas of interest from this study: (a) what effect does stress have on the paleomagnetic direction of a rock and (b) what effect does stress have on the magnetization intensity of a sample? To address this we need to look beyond the response of individual particles, to consider assemblages of particles with different orientations.

Rocks contain thousands or millions of magnetic particles (Berndt et al., 2016); the response of an assemblage of particles can be quite different to that of individual particles. To address this we consider the effect of distributions of particles of different sizes and initial domain states. We consider four groupings (a) SD behavior only, (b) transdomain behavior, (c) SV behavior only, and (d) all three groups combined (SD + SV + trans) (Figure 4). This study does not attempt to model all possible domain states, sizes and ARs. The simulations are skewed to more "interesting" complex states, particularly near the SD-SV transition size (Figure 1). Consequently, the response of the assemblages are indicative of trends and not exhaustive. However, to account for the favorability or likelihood of a given state, where more than one initial state exists for a given particle size and AR, for example, 100 nm and AR = 0.67 (Figure 3), when averaging, the models were added together by their probability of existing determined using their initial energies and the Boltzmann partition function. In addition, the volume was not accounted for during averaging, that is, all the particles' magnetizations were normalized and weighted equally. This favors the smaller particles, though typically smaller particles are more abundant in rocks. As the stress fields were applied over an octant, each assemblage of 20 stress orientations for a given initial magnetization had a non-zero magnetization once the magnetizations had been summed in the stress-field reference frame. Averaging the magnetizations of different particles in a common stress-field reference frame gave rise to a non-zero magnetization, equivalent to a non-saturating isothermal remanent magnetization. The orientation of these average magnetizations in the stress-field reference frame was arbitrary (Figure 4), however, in all four cases the mean direction was initially orientated between 34° and 47° from the compression stress axis.

The response of the SD-only particle's net magnetic direction is to rotate away from the stress axis (z-axis) as seen in Figure 4. The effect is more pronounced in the "under stress" equal area plot than the "zero stress" plot,

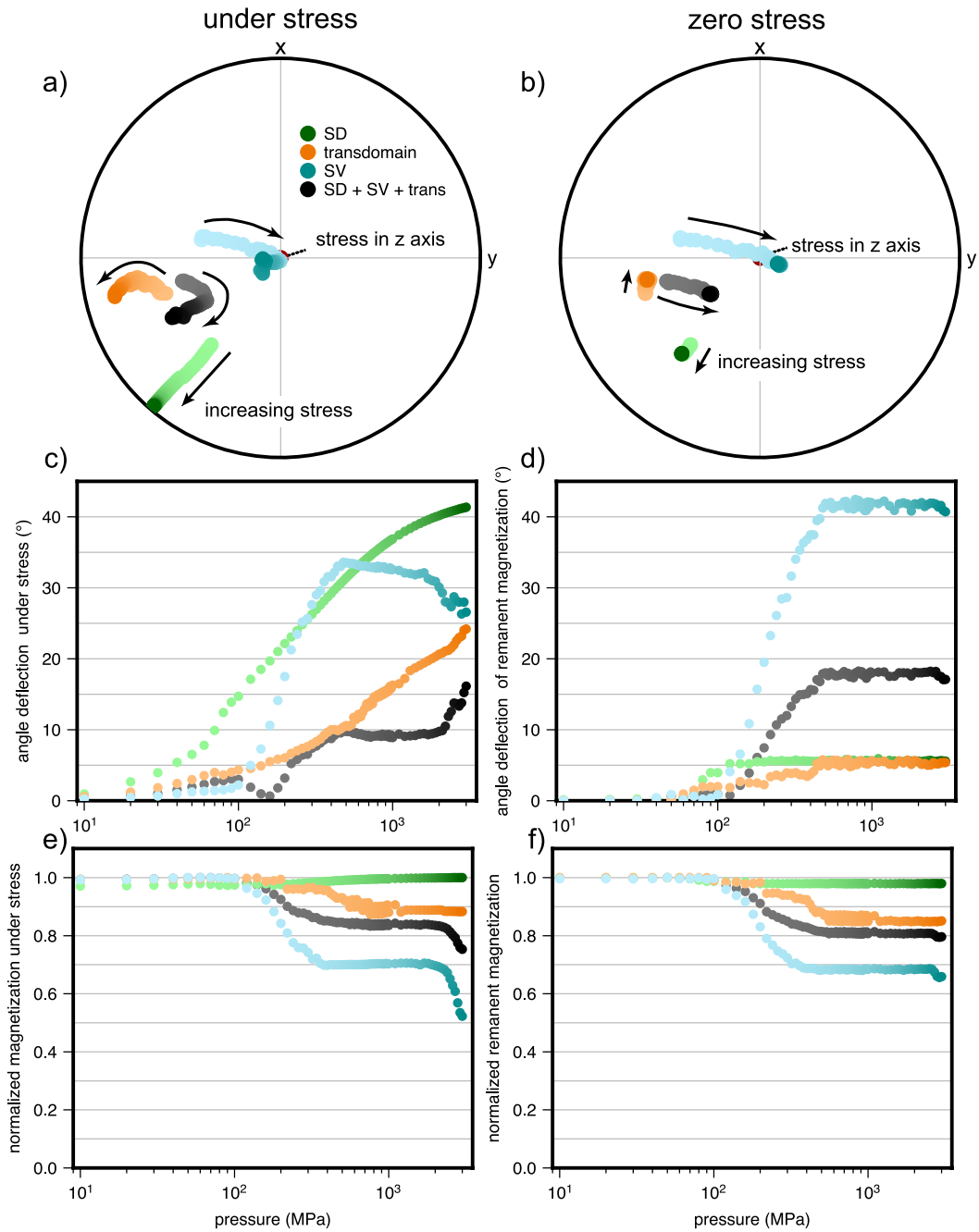

Figure 4. Magnetic response of assemblages of particles grouped by behavior: assemblages of exclusively single domain (SD) (80 particles) or single vortex (SV) (240 particles) behavior, assemblages which displayed some transdomain behavior (200 particles) and all the models in the study combined, that is, SD, SV and transdomain. In panels (a, b) the response of the four assemblages' mean directions to increasing stress are plotted on equal-area plots. In panel (a), the assemblages are under stress, and in panel (b) the response of the same assemblages after the stress is relaxed. The stress was applied along the *z*-axis (red circle), and all the data are in the same hemisphere. In panels (c, d) the angular deviation in the net magnetizations' directions are plotted as a function of stress both under stress (c) and after the stress is released (d). In panels (e, f) the normalized magnetizations, that is, intensity are plotted as a function of increasing stress. In panel (e) the magnetization is under stress, and (f) the magnetization is after the stress has been relaxed, that is, the zero-stress state. The color scheme in panels (a, b) corresponds to the colors in panels (c–f). For the purposes of averaging, where more than one initial model exists for a given particle size and morphology, for example, 100 nm and aspect ratio = 0.67 (Figure 3), the models were added together by their probability of existing determined using the Boltzmann partition function. Volume was not account for during averaging, that is, all the particles' magnetizations were normalized and weighted equally.

as much of much the SD behavior is reversible. For the SD grouping, σ_c is 85 MPa, that is, not many particles re-orient with the application of stress, but the ones that do, do so at relatively low stresses. In contrast the SV-only particles display quite a different response. First, the net magnetization direction rotates toward and aligns with the stress axis, and second this behavior is irreversible, that is, the "zero stress" state (Figures 4b and 4d) is increasingly aligned with the stress axis. σ_c is a little higher than the SD grouping at 100 MPa. The transdomain grouping's behavior is quite similar to the SD response, that is, the net magnetization rotates away from the stress axis, and is essentially reversible after the removal of stress (Figures 4b and 4d). σ_c is the highest at 220 MPa. The combination of all three groupings, leads to a mixed response, with a reversible rotation away from the stress axis not observed in the "zero stress" trend, but an irreversible "SV rotation" toward the stress axis. σ_c is 140 MPa for all the data combined.

In terms of net magnetization intensity, the SD-only grouping were close to invariant to stress both during stress application and after release (Figures 4e and 4f). In contrast, the SV-only and the transdomain groupings, plus the combination of all three groupings, display irreversible decreases in the magnetization between 100 and 300 MPa of up to ∼30%, that is, the magnetization intensity decreases with increasing stress. The effect is most pronounced in the SV-only grouping, which also displays a second mostly reversible drop in the magnetization intensity above 2,000 MPa (Figure 4f).

4.2. Comparison to Analytical SD Theory

Analytical calculations for the effect of stress on SD particles typically focus on elongated SD particles with uniaxial anisotropy, that is, so called Stoner and Wohlfarth (1948) particles (SW, e.g. Hodych, 1976, 1977). For assemblages of ideal SW particles, only stress fields aligned exactly perpendicular to the elongation axis above a critical value of stress, will be able to cause irreversible rotations, that is, changes to the zero-stress state, in the absence of any magnetic fields. Stress aligned at any other angle will simply cause a momentary and reversible deflection of the grains' magnetization whilst stress is applied. For the perpendicular-aligned SW particles, after the application of stress there is a 50% chance that they will re-align with their initial orientation, that is, an effective demagnetization for an assemblage of perpendicularly aligned SW particles. However, for random distributions of SW particles, effectively no particles will have this exact perpendicular configuration, in effect meaning that the remanence of random assemblages of ideal SW particles will be unaffected by stress applied in the absence of external magnetic fields.

In reality, SD particles in rocks are not ideal SW particles. SD particles can be near-equant and controlled by the magnetocrystalline anisotropy, or irregular with triaxial or higher order anisotropy (Nikolaisen et al., 2020). In such cases, they are unlikely to display the high-levels of symmetry seen in ideal SW particles and may display configurational anisotropy (Williams et al., 2006). This micromagnetic study includes the contributions of both the magnetocrystalline anisotropy and any configurational anisotropy, however, the models are all symmetric about their principal <100> axes (Figure 2). The SD models for the elongated particles, that is, AR = 0.67 or 0.5, essentially agree with SW theory predictions. The SD model for equant particles, that is, 50 nm EVSD with AR = 1.0, shows irreversible behavior on the application of stress due to the higher magnetocrystalline anisotropy symmetry (Figures 2a–2c and 3). Stresses between 90 and 150 MPa are sufficient to cause most of the irreversible changes; the range being dependent on the relative orientation of the stress fields and particle. These stresses are lower than predicted by analytical SD theory for SW particles. Using Equation 1 we can determine when the stress energy overcomes the shape anisotropy energy. This occurs at about ∼500 MPa, however, this value depends on the relative orientation of the particle with respect to the particle orientation. For certain orientations this can be ≫1 GPa; therefore for random distributions, stresses of >1 GPa are required. Compared to analytical models (e.g., Hodych, 1976, 1977) micromagnetic models for SD particles predict that lower stresses are needed to cause irreversible magnetization behavior.

4.3. Implications for Paleomagnetic Studies

There have been many studies which have investigated the effect of differential stress on the magnetization of rocks, many of which have showed that changes in remanent (zero-stress state) magnetization occur at stresses ≪1 GPa (e.g., Hamano et al., 1989; Nagata, 1971; Sato et al., 2021; Volk & Gilder, 2016). The mismatch between SD theory based on SW particles and experiment is well documented, with differences being associated to the SV

or MD effects (Volk & Feinberg, 2019). Most studies have analyzed real rocks, where particle sizes are poorly constrained.

This micromagnetic study demonstrates that SV particles—and equant SD particles—can display significant changes in magnetization at stresses of only ∼100 MPa (Figure 3), thereby aligning theory and experiment. We have shown that these changes below 1 GPa are a true SV phenomena, and are not due to very large, geologically unstable MD particles. This is important because it is now thought that SV remanences are more stable on geological timescales than SD remanences, particularly in equant particles (Nagy et al., 2017, 2022). Hence, it is actually SV particles that dominate the magnetic remanence of rocks. This leads to a stability dichotomy: SV particles are more thermally stable than SD particles, but are less stable to the effect of stress.

It may be argued that a threshold of $\sigma_c \geq 3°$ is too low, however, there are many paleomagnetic studies where such accuracy is required, for example, in high-resolution time-averaged-field studies (e.g., Johnson et al., 2008).

Differential stresses of ∼100 MPa are common near earthquake zones, during tectonic mountain building and during impacts (Lambert & Lapusta, 2023; North, Collins, et al., 2023). This new knowledge can be seen both positively and negatively. For example, in earthquake zones, this new knowledge opens up the possibility of using paleomagnetic signals near earthquake zones, to be used as paleo-stress indicators. However, in plate tectonic reconstructions maybe compromised as paleomagnetic directional information as stresses of ∼100 MPa are common. Similarly, ancient magnetic field intensity (paleointensity) estimates maybe underestimated, as stresses of ∼100 MPa reduce the net magnetization by 20%–30% (Figure 4). This is particularly likely in meteoritic samples, as meteorites may have experienced multiple impacts in their history (Steele et al., 2023), and where the stresses are too low, that is, <5 GPa, to be accurately recorded petrographically (Scott et al., 1992).

5. Conclusions

We have shown that the magnetic response of SV particles to differential compressive stress is the exact opposite of SD particles (Figures 2 and 4). That is, the net magnetic moment of SV particles rotates toward the compression axis, whereas that of SD particles rotates away from the compression axis. The models for elongated SD particles in this paper are in agreement with analytical SD theories (e.g., Hodych, 1976, 1977). We also demonstrate that stress can also change the domain states of particles near the SD to SV transition size, depending on the initial magnetization state.

The micromagnetic models for SV and equant SD particles indicate that far lower compressive stresses are required to cause significant, that is, >3°, changes to their magnetization directions and intensities. For assemblages of particles, stresses of only ∼100 MPa are required, compared to analytical estimates based on SW theory of ∼1,000 MPa. For the same stresses, paleointensities may also reduced by ∼30% (Figure 4). Such effects will need to be considered when interpreting both paleomagnetic direction and intensity in future studies; however, this new knowledge opens up the possibility of using paleomagnetic signals as paleo-stress indicators, for example, in earthquake zones.

Data Availability Statement

All results reported here were generated using the open source micromagnetic modeling code of Ó Conbhuí et al. (2018). The input scripts, geometries and initial starting states (see Supporting Information S1) used to construct these models in the paper are available at North, Muxworthy, et al. (2023).

Acknowledgments
T.L.N. acknowledges a STFC-funded PhD studentship (ST/S505420/1). A.R.M. and W.W. acknowledge funding from NERC (NE/V001388/1).

References

Almeida, T. P., Muxworthy, A. R., Kovacs, A., Williams, W., Brown, P. D., & Dunin-Borkowski, R. E. (2016). Direct visualization of the thermomagnetic behavior of pseudo-single-domain magnetite particles. *Science Advances*, *2*(4), e1501801. https://doi.org/10.1126/sciadv.1501801

Berndt, T., Muxworthy, A. R., & Fabian, K. (2016). Does size matter? Statistical limits of paleomagnetic field reconstruction from small rock specimens. *Journal of Geophysical Research: Solid Earth*, *121*(1), 15–26. https://doi.org/10.1002/2015jb012441

Biggin, A. J., Piispa, E. J., Pesonen, L. J., Holme, R., Paterson, G. A., Veikkolainen, T., & Tauxe, L. (2015). Palaeomagnetic field intensity variations suggest Mesoproterozoic Inner-Core nucleation. *Nature*, *526*(7572), 245–248. https://doi.org/10.1038/nature15523

Coreform LLC. (2017). Coreform Cubit, v16.4 (64-bit). Retrieved from https://coreform.com

Dunlop, D. J., Newell, A. J., & Enkin, R. J. (1994). Transdomain thermoremanent magnetization. *Journal of Geophysical Research*, *99*(B10), 19741–19755. https://doi.org/10.1029/94JB01476

Dunlop, D. J., Ozima, M., & Kinoshita, H. (1969). Piezomagnetization of single-domain grains: A graphical approach. *Journal of Geomagnetism and Geoelectricity*, *21*(2), 513–518. https://doi.org/10.5636/jgg.21.513

Elhanati, D., Levi, T., Marco, S., & Weinberger, R. (2020). Zones of inelastic deformation around surface ruptures detected by magnetic fabrics. *Tectonophysics*, *788*, 228502. https://doi.org/10.1016/j.tecto.2020.228502

Enkin, R. J., & Williams, W. (1994). Three-dimensional micromagnetic analysis of stability in fine magnetic grains. *Journal of Geophysical Research*, *99*(B1), 611–618. https://doi.org/10.1029/93JB02637

Fabian, K., & Heider, F. (1996). How to include magnetostriction in micromagnetic models of titanomagnetite grains. *Geophysical Research Letters*, *23*(20), 2839–2842. https://doi.org/10.1029/96GL01429

Fabian, K., Kirchner, A., Williams, W., Heider, F., Leibl, T., & Hubert, A. (1996). Three-dimensional micromagnetic calculations for magnetite using FFT. *Geophysicsal Journal International*, *124*(1), 89–104. https://doi.org/10.1111/j.1365-246X.1996.tb06354.x

Hamano, Y., Boyd, R., Fuller, M., & Lanham, M. (1989). Induced susceptibility anisotropy of igneous rocks caused by uniaxial compression. *Journal of Geomagnetism and Geoelectricity*, *41*(2), 203–220. https://doi.org/10.5636/jgg.41.203

Hodych, J. P. (1976). Single-domain theory for the reversible effect of small uniaxial stress upon the initial magnetic susceptibility of rock. *Canadian Journal of Earth Sciences*, *13*(9), 1186–1200. https://doi.org/10.1139/e76-120

Hodych, J. P. (1977). Single-domain theory for reversible effect of small uniaxial stress upon the remanent magnetization rock. *Canadian Journal of Earth Sciences*, *14*(9), 2047–2061. https://doi.org/10.1139/e77-175

Johnson, C. L., Constable, C. G., Tauxe, L., Barendregt, R., Brown, L. L., Coe, R. S., et al. (2008). Recent investigations of the 0-5 Ma geomagnetic field recorded by lava flows. *Geochemistry, Geophysics, Geosystems*, *9*(4), Q04032. https://doi.org/10.1029/2007GC001696

Kapička, A. (1992). Magnetic-susceptibility under hydrostatic-pressure of synthetic magnetite samples. *Physics of the Earth and Planetary Interiors*, *70*(3–4), 248–252. https://doi.org/10.1016/0031-9201(92)90191-W

Lambert, V., & Lapusta, N. (2023). Absolute stress levels in models of low-heat faults: Links to geophysical observables and differences for crack-like ruptures and self-healing pulses. *Earth and Planetary Science Letters*, *618*, 118277. https://doi.org/10.1016/j.epsl.2023.118277

Moskowitz, B. M. (1993). High-temperature magnetostriction of magnetite and titanomagnetites. *Journal of Geophysical Research*, *98*(B1), 359–371. https://doi.org/10.1029/92JB01846

Muxworthy, A. R., & Williams, W. (2006). Critical single-domain/multidomain grain sizes in noninteracting and interacting elongated magnetite particles: Implications for magnetosomes. *Journal of Geophysical Research*, *111*(B12), B12S12. https://doi.org/10.1029/2006jb004588

Nagata, T. (1971). Introductory notes on shock remanent magnetization and shock demagnetization of igneous rocks. *Pure and Applied Geophysics*, *89*(1), 159–177. https://doi.org/10.1007/BF00875213

Nagy, L., Williams, W., Muxworthy, A. R., Fabian, K., Almeida, T. P., Ó Conbhuí, P., & Shcherbakov, V. P. (2017). Stability of equidimensional pseudo-single-domain magnetite over billion-year timescales. *Proceedings of the National Academy of Sciences of the United States of America*, *114*(39), 10356–10360. https://doi.org/10.1073/pnas.1708344114

Nagy, L., Williams, W., Tauxe, L., & Muxworthy, A. R. (2019). From nano to micro: Evolution of magnetic domain structures in multidomain magnetite. *Geochemistry, Geophysics, Geosystems*, *20*(6), 2907–2918. https://doi.org/10.1029/2019gc008319

Nagy, L., Williams, W., Tauxe, L., & Muxworthy, A. R. (2022). Chasing tails: Insights from micromagnetic modeling for thermomagnetic recording in non-uniform magnetic structures. *Geophysical Research Letters*, *49*(23), e2022GL101032. https://doi.org/10.1029/2022GL101032

Néel, L. (1949). Théorie du traînage magnétique des ferromagnétique en grains fins avec applications aux terres cuites. *Annales de Geophysique*, *5*, 99–136. https://doi.org/10.1051/jphysrad:0195000110204900

Nikolaisen, E. S., Harrison, R. J., Fabian, K., & McEnroe, S. A. (2020). Hysteresis of natural magnetite ensembles: Micromagnetics of silicate-hosted magnetite inclusions based on focused-ion-beam nanotomography. *Geochemistry, Geophysics, Geosystems*, *21*(11), e2020GC009389. https://doi.org/10.1029/2020gc009389

North, T. L., Collins, G. S., Davison, T. M., Muxworthy, A. R., Steele, S. C., & Fu, R. R. (2023). The heterogeneous response of martian meteorite Allan Hills 84001 to planar shock. *Icarus*, *390*, 115322. https://doi.org/10.1016/j.icarus.2022.115322

North, T. L., Muxworthy, A. R., Williams, W., Mitchell, T. M., Collins, G. S., & Davison, T. M. (2023). The effect of stress on paleomagnetic signals: A micromagnetic study of magnetite's single-vortex response [Dataset]. Zenodo. https://doi.org/10.5281/zenodo.8428674

Ó Conbhuí, P., Williams, W., Fabian, K., Ridley, P., Nagy, L., & Muxworthy, A. R. (2018). Merrill: Micromagnetic earth related robust interpreted language laboratory. *Geochemistry, Geophysics, Geosystems*, *19*(4), 1080–1106. https://doi.org/10.1002/2017gc007279

Sato, M., Kurosawa, K., Kato, S., Ushioda, M., & Hasegawa, S. (2021). Shock remanent magnetization intensity and stability distributions of single-domain titanomagnetite-bearing basalt sample under the pressure range of 0.1–10 GPa. *Geophysical Research Letters*, *48*(8), e2021GL092716. https://doi.org/10.1029/2021GL092716

Schmidbauer, E., & Petersen, N. (1968). Some magnetic properties of two basalts under uniaxial compression measured at different temperatures. *Journal of Geomagnetism and Geoelectricity*, *20*(3), 169–180. https://doi.org/10.5636/jgg.20.169

Scott, E. R., Keil, K., & Stöffler, D. (1992). Shock metamorphism of carbonaceous chondrites. *Geochimica et Cosmochimica Acta*, *56*(12), 4281–4293. https://doi.org/10.1016/0016-7037(92)90268-N

Steele, S. C., Fu, R. R., Volk, M. W., North, T. L., Brenner, A. R., Muxworthy, A. R., et al. (2023). Paleomagnetic evidence for a long-lived, potentially reversing martian dynamo at 3.9 Ga. *Science Advances*, *9*(21), eade9071. https://doi.org/10.1126/sciadv.ade9071

Stoner, E. C., & Wohlfarth, E. P. (1948). A mechanism of magnetic hysteresis in heterogeneous alloys. *Philosophical Transactions of the Royal Society of London*, *240*(4), 599–642. https://doi.org/10.1109/TMAG.1991.1183750

Volk, M. W. R., & Feinberg, J. M. (2019). Domain state and temperature dependence of pressure remanent magnetization in synthetic magnetite: Implications for crustal remagnetization. *Geochemistry, Geophysics, Geosystems*, *20*(5), 2473–2483. https://doi.org/10.1029/2019gc008238

Volk, M. W. R., & Gilder, S. A. (2016). Effect of static pressure on absolute paleointensity recording with implications for meteorites. *Journal of Geophysical Research: Solid Earth*, *121*(8), 5596–5610. https://doi.org/10.1002/2016jb013059

Williams, W., & Dunlop, D. J. (1989). Three-dimensional micromagnetic modelling of ferromagnetic domain structure. *Nature*, *377*(6208), 634–637. https://doi.org/10.1038/337634a0

Williams, W., Muxworthy, A. R., & Paterson, G. A. (2006). Configurational anisotropy in single-domain and pseudosingle-domain grains of magnetite. *Journal of Geophysical Research*, *111*(B12), B12S13. https://doi.org/10.1029/2006jb004556